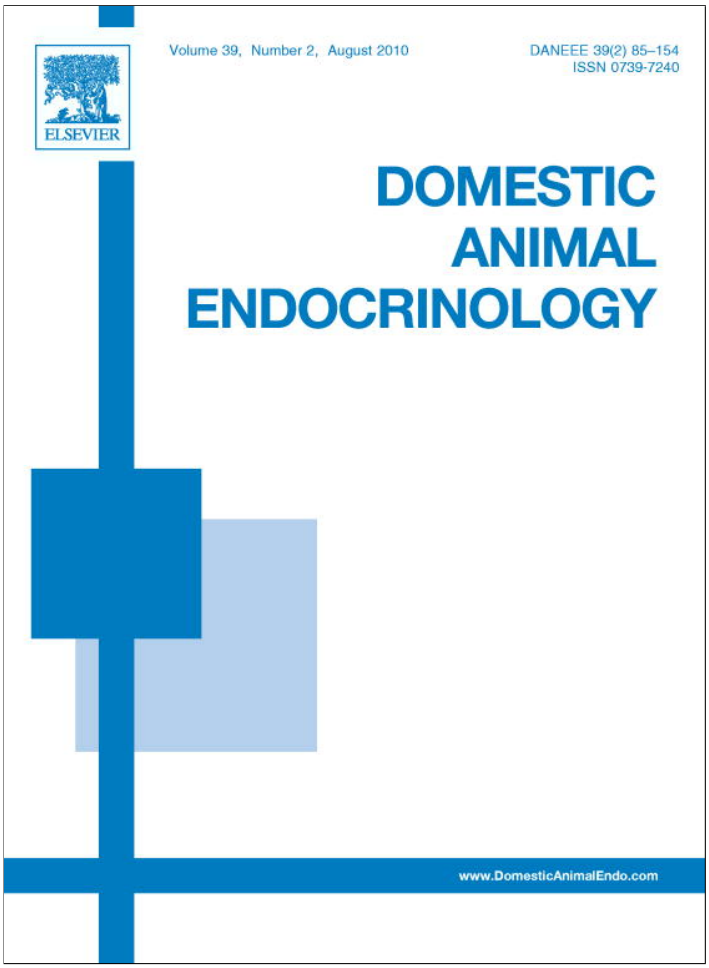

Available online at www.sciencedirect.com
ScienceDirect
Domestic Animal Endocrinology 39 (2010) 116–130
DOMESTIC ANIMAL ENDOCRINOLOGY
www.domesticanimalendo.com

Expression of luteal estrogen receptor, interleukin-1, and apoptosis-associated genes after $PGF_{2\alpha}$ administration in rabbits at different stages of pseudopregnancy

M. Maranesi[a], M. Zerani[c], L. Lilli[a], C. Dall'Aglio[b], G. Brecchia[a], A. Gobbetti[d], C. Boiti[a,*]

[a] *Department of Veterinary Biopathological Science, Laboratory of Biotechnology, Section of Physiology, University of Perugia*
[b] *Section of Anatomy, University of Perugia*
[c] *School of Veterinary Medicine Science, University of Camerino, Matelica*
[d] *School of Bioscence and Biotechnology, University of Camerino, Italy*

Abstract

The dynamic expression for estrogen receptor subtype-1 (ESR1), interleukin-1β (IL1B), and apoptosis-associated genes, as well as nitric oxide synthase activity, were examined in corpora lutea (CL) of rabbits after prostaglandin $F_{2\alpha}$ ($PGF_{2\alpha}$) administration on either day 4 or day 9 of pseudopregnancy. By reverse transcriptase polymerase chain reaction, the steady-state level of *ESR1* transcript was lower ($P < 0.01$) and that of anti-apoptotic B-cell CLL/lymphoma 2 (*BCL2*) -like 1 (*BCL2L1*) was greater in day 4 ($P < 0.01$) than in day 9 CL. Western blot analysis revealed that BCL2-associated X protein (BAX) abundance was greater in day 4 ($P < 0.01$) than in day 9 CL, whereas BCL2L1 protein was undetectable at both luteal stages. After $PGF_{2\alpha}$, *ESR1* transcript decreased ($P < 0.01$) in day 9 CL, whereas *IL1B* mRNA showed a transitory increase ($P < 0.01$) at both stages. The pro-apoptotic tumor protein p53 (*TP53*) gene had diminished ($P < 0.01$) on day 4 and on day 9 after a transitory increase ($P < 0.01$), whereas the *BAX*/*BCL2L1* expression ratio increased ($P < 0.01$) in day 9 CL 24 h after treatment. Following $PGF_{2\alpha}$, TP53 protein increased ($P < 0.01$) at both luteal stages, and BAX decreased ($P < 0.01$) in day 4 CL but increased ($P < 0.01$) 24 h later in day 9 CL; BCL2L1 became detectable 6 h later in day 4 CL. Nitric oxide synthase activity temporarily increased ($P < 0.01$) following $PGF_{2\alpha}$. These findings suggest that $PGF_{2\alpha}$ regulates luteolysis by *ESR1* mRNA down-regulation and modulation of pro- and anti-apoptotic pathways in CL that have acquired a luteolytic capacity.

Keywords: ESR1; IL1B; TP53; BAX; BCL2L1; Luteolysis

1. Introduction

In rabbits, as in many other species, luteal regression after an infertile mating or at the end of gestation is driven by prostaglandin $F_{2\alpha}$ ($PGF_{2\alpha}$) of uterine origin [1]. Recently, several distinct intraluteal pathways have emerged as potential candidate mediators of the initial $PGF_{2\alpha}$ triggering action [2], including nitric oxide synthase (NOS) [3,4], endothelial-derived factors endothelin-1 [5] and angiotensin II [6], as well as locally synthesized PGs [7]. Though the $PGF_{2\alpha}$-dependent functional processes have also received much attention in corpora lutea (CL) of sows [8] and cows [9], the underlying cellular mechanism and the timing of its

* Address correspondence to: Department of Veterinary Biopathological Science, University of Perugia, S. Costanzo 4, I-06126 Perugia, Italy; Phone: +39-075-5857639; Fax: +39-075-5857654.
E-mail: cristiano.boiti@unipg.it (C. Boiti).

0739-7240/10/$ – see front matter © 2010 Elsevier Inc. All rights reserved.
doi:10.1016/j.domaniend.2010.03.001

induction are still unclear in rabbits, and little is known about what factors confer luteolytic capacity to exogenous $PGF_{2\alpha}$ administered in the mid-luteal stage of pseudopregnancy [10].

In this context, it is likely that IL1, together with several other cytokines normally found in rabbit CL [11,12], are involved in the control of luteal function acting locally as pro-inflammatory mediators leading to apoptosis [13]. Similarly, little is known about the subtle interplay with locally acting hormones and intraluteal factors exhibiting both pro- and anti-apoptotic properties, which may be regulated dynamically. In rabbits, estradiol-17β is recognized as the main luteotrophic hormone because its withdrawal leads to functional luteolysis owing to activation of apoptosis [14]. In addition, NOS and its product NO have been shown to have both pro- and anti-apoptotic effects through modulation of several intracellular pathways including B-cell CLL/lymphoma 2 (BCL2) and tumor protein p53 (TP53) proteins [15], but in the rabbit, CL inhibition of NOS favors apoptosis [16].

Therefore, the main objective of the present study was to elucidate the temporal changes in expression of genes and proteins associated with apoptosis in CL from early (day 4) and mid (day 9) pseudopregnancy in response to $PGF_{2\alpha}$ to improve our understanding of their role in the acquisition of age-dependent luteolytic capacity. To this end, experiments were devised to characterize, at each luteal stage, the expression for estrogen receptor, subtype-1 (ESR1), interleukin-1β (IL1B), TP53, BCL2-associated X protein (BAX), and BCL2-like 1 (BCL2L1) following $PGF_{2\alpha}$ challenge as well as the enzymatic activity of NOS.

2. Materials and methods

2.1. Reagents

Random hexamer primers, deoxyribonuclease I (DNAase I Amp. Grade), RNAse H- reverse transcriptase (SuperScript III Reverse Transcriptase), *E. coli* RNase H, and DNA ladders were obtained from Invitrogen (S. Giuliano Milanese, Milan, Italy), as well as reagent for isolation and purification of total RNA (TRIzol), Taq DNA polymerase (Platinum), 10× PCR Buffer, 50 mM $MgCl_2$, RNAse-free tubes and RNAse-free water, and deoxy-NTPs. Primers for *18S* rRNA and corresponding competimers (QuantumRNA 18S Internal Standards) were acquired from Applied Biosystems (Monza, MI, Italy). Primers for mRNAs of *IL1B*, *ESR1*, *TP53*, *BCL2L1*, and *BAX* were supplied by Invitrogen. A Nucleospin Extract II kit was purchased from Macherey Nagel Inc. (Bethlehem, PA, USA). Tritiated [2,3-3H]L-arginine, with a specific activity of 30–40 Ci/mmol, was purchased from Amersham Biosciences (Amersham Biosciences Ltd, Little Chalfont, Bucks, UK). The NOS detect assay kit was purchased from Alexis Corp. (Läufelfingen, Switzerland). The kit for the protein assay was purchased from Bio-Rad Laboratories (Hercules, CA, USA). The primary monoclonal antibody mouse anti-ESR1 used for immunohistochemistry (IHC) was supplied by Zymed (San Francisco, CA, USA). The mouse monoclonal antibodies anti-TP53 (sc-73566), BAX (sc-7480), and BCL2L1 (sc-8392), used for IHC and Western blot (WB) analyses were purchased from Santa Cruz Biotechnology (Santa Cruz, CA, USA). The mouse monoclonal anti-β-tubulin antibody was from Sigma-Aldrich (St.Louis, MO, USA). The biotinylated secondary antibody (goat anti-mouse IgG) used for IHC was purchased from Vector Laboratories (Burlingame, CA, USA). The avidin-biotin complex (ABC, Vector Elite Kit) and the chromogen 3,3′-diaminobenzidine tetrachloride (DAB) were acquired from Vector Laboratories. PageRuler Protein Ladder for WB was obtained from Fermentas (Burlington, Ontario, Canada). The horseradish peroxidase (HRP)-conjugated rabbit anti-mouse IgG secondary antibody, used for WB as the Restore Western blot stripping buffer, was obtained from Thermo Fisher Scientific (Rockford, IL, USA). Protran nitrocellulose membranes were purchased from Whatman (Dassel, Germany). Biomax films used to document immunocomplexes were acquired from Kodak Laboratories (Rochester, NY, USA). The enhanced chemiluminescence detection system for WB (Immobilon Western Chemiluminescent HRP Substrate) was purchased from Millipore (Billerica, MA, USA). The bands were quantified using Quantity One software, version 4.6.3 (Bio-Rad Laboratories, Hercules, CA, USA, 2009). All other pure-grade chemicals and reagents were obtained locally.

2.2. Animals, hormonal regimen, and tissue collection

The protocols involving the care and use of the animals for these experiments were approved by the Bioethics Committee of the University of Perugia. Unmated 5-mo-old New Zealand white rabbits, weighing 3.5–3.8 kg, were caged individually in quarters of the University of Perugia Central Animal Facility and maintained under controlled conditions of light (14 h light: 10 h dark) and temperature (18 °C). The animals were provided with commercial rabbit chow and tap water *ad libitum*. All rabbits were treated with 20 IU

eCG, followed 2 d later by an i.m. injection of 0.8 μg of GnRH to induce pseudopregnancy. The day of GnRH injection was designated day 0.

On day 4 or day 9 of pseudopregnancy, rabbits (n = 18/group) were administered 200 μg alfaprostol by i.m. injection. At each luteal stage, 3 rabbits were killed by cervical dislocation just before (time 0) and then 1.5, 3, 6, 12, and 24 h after $PGF_{2\alpha}$. Reproductive tracts, promptly removed from each animal, were thoroughly washed with saline. Within a few minutes, after rinsing with RNAse-free phosphate buffered saline for later evaluation of gene and protein expression, the CL were excised from the ovaries and, after careful dissection of nonluteal tissue using fine forceps under stereoscopic magnification, immediately frozen at −80 °C. For the immunohistochemical detection of ESR1, TP53, BAX, and BCL2L1, 2 additional animals for each time point were sacrificed just prior (time 0) and 6 h after $PGF_{2\alpha}$ injection administeredon either day 4 or day 9 of pseudopregnancy. The ovaries, excised immediately after sacrifice, were fixed by immersion in 4% (w/v) formaldehyde in phosphate-buffered saline (PBS, pH 7.4) for 24 h at room temperature and subsequently processed for embedding in paraffin following routine tissue preparation procedures.

From each rabbit, 3 blood samples were collected by venous puncture of the marginal ear vein: the first, just before GnRH treatment; the second, before $PGF_{2\alpha}$ injection, and the third immediately prior to sacrifice. The samples, collected in EDTA vacutainers, were centrifuged at 3000 × *g* for 15 min, and the plasma was stored frozen until assayed for progesterone concentrations to assess the functional status of the ovarian CL. For the purpose of this work, functional luteolysis was defined as a 50% drop of plasma progesterone from pretreatment values, before $PGF_{2\alpha}$ administration, and complete luteolysis as the failure of CL to secrete progesterone so that blood concentrations fall below 1.0 ng/mL, which is the concentration found in estrous rabbits.

2.3. Immunohistochemistry of ESR1, TP53, BAX, and BCL2L1

The immunohistochemical procedure was performed on serial 5 μm-thick sections of the ovaries to identify the cell localization of ESR1, TP53, BAX, and BCL2L1 using the corresponding primary monoclonal mouse antibodies diluted 1:80, 1:100, 1:100, and 1:100, respectively, followed by the biotinylated secondary antibody (1:200) according to protocols already described [17]. Sections in which the primary antibodies were omitted or substituted by pre-immune mouse gamma globulin were used for the negative controls of nonspecific staining.

The intensity of immunostaining was conventionally classified as being absent, weak, moderate, and strong when, respectively, <1%, 1%–10%, 10%–50%, 50%–100% of the cells in the CL section per field of vision using light microscopy stained positively.

2.4. RNA extraction and reverse transcription

For each rabbit, total RNA was extracted from a pool of CL, as previously described [12]. Genomic DNA contamination was prevented by treatment with deoxyribonuclease I according to instructions. According to the protocol provided by the manufacturer, 5 μg of total RNA were reverse-transcribed in 20 μL of SuperScript III Reverse Transcriptase cDNA synthesis mix using random hexamers. Genomic DNA contamination was checked by developing the PCR procedure without reverse transcriptase.

2.5. Multiplex RT-PCR amplification

Multiplex PCR amplification was carried out as previously described [12] using 1 μL of luteal cDNA as template for targets and *18S* primers (Table 1). Cycling conditions consisted of an initial denaturizing cycle at 94 °C for 75 sec, followed by a variable number of cycles for each target gene (Table 1) at 94 °C for 15 sec, 60 °C for 30 sec, 72 °C for 45 sec, and a final extension step at 72 °C for 10 min. Within each experiment and for each gene analyzed, the complete set of samples was processed in parallel in a single polymerase chain reaction (PCR), using aliquots of the same PCR master mix. The amplified PCR-generated products (20 μL of 25 μL total reaction volume) were

Table 1
Primers for *ESR1*, *IL1B*, *TP53*, *BAX*, *BCL2L1*, and *18S* used as internal standard.

Gene	Product size (bp)	Primers (5′-3′)	Cycles (no.)
ESR1	147	F-AGATCCAAGGGAATGAGCTG R-CTGCGGCGTTGAACTCATA	35
IL1B	183	F-TGAGGCCGATGGTCCCAATTA R-AAGGCCTGTGGGCAGGGAAC	35
TP53	300	F-GCTGCTCCGACAGCGATGGT R-CCCTCCCAGGACAGGCACAC	30
BAX	165	F-CCTTTTGCTTCAGGGTTTCA R-ATCCTCTGCAGCTCCATGTT	32
BCL2L1	228	F-ACAGCAGTGAAGCAGGCTCT R-CATCTCCTTGTCCACGCTTT	30
18S	489	F-TCAAGAACGAAAGTCGGAGGTT R-GGACATCTAAGGGCATCA	

analyzed by electrophoresis on 2% agarose gel using ethidium bromide staining. Analysis of amplification products was carried out as reported elsewhere [12]. The amplified products, collected from agarose gel after electrophoresis, were purified with Nucleospin Extract II kit and their identity confirmed by DNA sequencing using Sanger's method.

2.6. Protein analysis of TP53, BAX, and BCL2L1 by Western blotting

The changes in expression of luteal TP53, BAX, and BCL2L1 proteins were analyzed by WB either before or after $PGF_{2\alpha}$ administration at both the early and mid-luteal stages. For each rabbit, total luteal proteins were extracted from a pool of 8 CL, as previously described [18]. Briefly, the CL were homogenized in 1 mL ice-cold RIPA buffer (PBS containing 1% Igepal CA-630, 0.5% sodium deoxycholate, and 0.1% SDS). After incubation at 4 °C for 20 min, the homogenates were centrifuged at 12,000 × *g* for 60 min at 4 °C. The protein concentrations of supernatants were measured using the protein assay kit with bovine serum albumin (BSA) as standard. Equivalent amounts of protein (20 μg) were separated by discontinuous 10% SDS-PAGE with 4% staking gel for 40 min at 200 V and 500 mA. Thereafter, proteins were transferred onto nitrocellulose membranes for 1 h at 100 V and 350 mA. Membranes were then blocked in Tris-buffered saline (TBS) containing 0.05% Tween 20, 5% nonfat dried milk, and 3% BSA. Immunoblotting was performed by sequential exposure to anti-TP53, anti-BAX, and anti-BCL2L1 monoclonal antibodies (1:500) overnight at 4 °C. Membranes were then probed with HRP-labeled rabbit anti-mouse IgG antibody (1:20,000) for 60 min at room temperature under gentle agitation. All antibody incubations were performed in TBS containing 5% nonfat dried milk and 0.05% Tween-20. The immunocomplexes were detected by enhanced chemiluminescence according to the manufacturer's protocol and exposed to x-ray film. Blot images were acquired, and the intensities of the bands were quantified by densitometric analysis. After the blots were stripped, membranes were reprobed with anti-μ-tubulin mouse monoclonal antibody (0.5 μg/mL) overnight at 4 °C, as above. Values were expressed as arbitrary units of relative abundance of the specific proteins normalized with that of β-tubulin used as loading control.

2.7. NO synthase activity determination

Nitric oxide synthase activity was determined by monitoring the conversion of [3H]L-arginine to [3H]L-citrulline with a commercial NOS assay kit, according to the experimental protocol described by Boiti et al [12].

2.8. Progesterone assay

Progesterone concentrations were determined by radioimmunoassay, using specific antibody according to the procedure reported elsewhere [3]. Progesterone was extracted from corresponding 0.1 mL plasma samples with ethyl ether, and each sample was assayed in duplicate. The assay sensitivity was 0.08 ng/mL for progesterone, whereas intra- and interassay coefficients of variation were 5.3% and 10.2%, respectively.

2.9. Statistical analysis

Data on gene and protein expression, progesterone plasma concentrations, and NOS activity were examined by ANOVA followed by the Student-Newman-Keuls *t* test. Data on the expression ratio of *BAX*/*BCL2L1* mRNAs were examined by the nonparametric Kruskal-Wallis test followed by the Student-Newman-Keuls *t* test. Differences were considered significant at $P < 0.01$.

3. Results

3.1. In vivo induction of luteolysis

Progesterone plasma concentration, used as a marker of luteal functional activity, was low (0.6 ± 0.3 ng/mL) in all does before induction of ovulation. Progesterone decreased 12 h ($P < 0.01$) after $PGF_{2\alpha}$ injection on day 9 of pseudopregnancy, and complete functional regression was achieved 24 h ($P < 0.01$) later, when it decreased to basal values found at estrus (Fig. 1). As expected, $PGF_{2\alpha}$ was ineffective in inducing a functional regression when administered on day 4 of pseudopregnancy.

3.2. Immunolocalization of ESR1, TP53, BAX, and BCL2L1

Using monoclonal antibodies, strong positive reaction for ESR1 was observed in the nucleus of luteal cells of both day 4 and day 9 CL before $PGF_{2\alpha}$ injection (Fig. 2, top panels). The intensity of immunostaining remained unaffected 6 h after $PGF_{2\alpha}$ treatment in day 4 CL, but it became moderate in day 9 CL (Fig. 2, top panels). Independently of luteal stage, moderate and strong nuclear immunopositivity for TP53 was detectable in luteal cells before and after treatment, respectively (Fig. 2, middle panels). Weak nuclear staining for BAX was detectable in luteal cells of both day 4 and

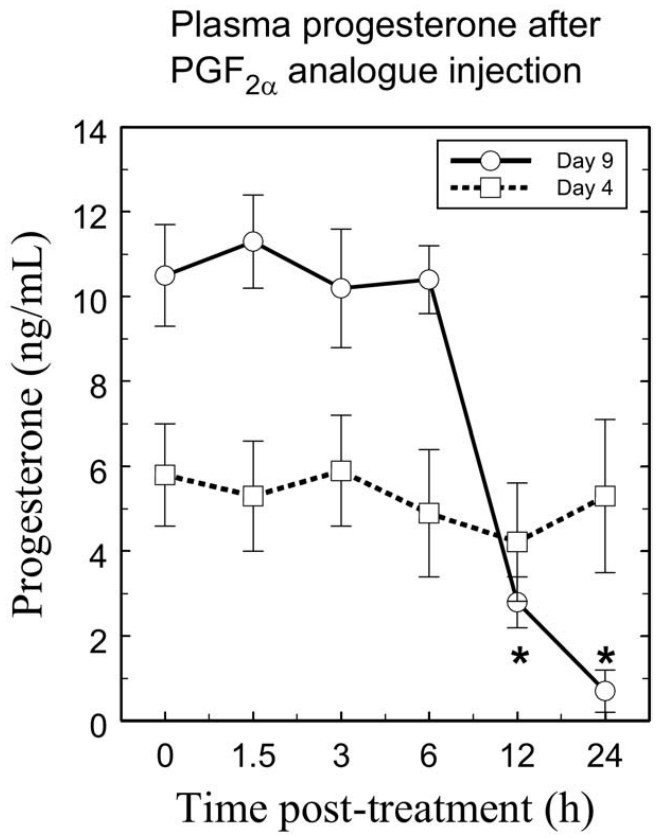

Fig. 1. Plasma progesterone concentrations in blood samples collected 0, 1.5, 3, 6, 12, and 24 h after $PGF_{2\alpha}$ analog injection on day 4 or day 9 of pseudopregnancy. Apart from time 0, each data point represents mean ± SD of values derived from 3 different rabbits. Asterisks indicate significantly different values ($P < 0.01$) from time 0 progesterone concentrations.

day 9 CL before and after $PGF_{2\alpha}$ injection (Fig. 2, bottom panels). Independently of luteal stage, no staining for BCL2L1 was observed in CL either before or after $PGF_{2\alpha}$ challenge (data not shown). Positive immunoreaction was detected in the ooplasm of oocytes (data not shown). Staining was absent when the corresponding primary antibodies were substituted with non-immune serum (data not shown).

3.3. Gene expression of ESR1 and IL1B

Before treatment, the steady-state level of CL *ESR1* mRNA was lower ($P < 0.01$) on day 4 than on day 9 of pseudopregnancy (Fig. 3). On day 4, the *ESR1* mRNA levels remained fairly constant during the 24 h following alfaprostol administration. Conversely, on day 9 of pseudopregnancy, the relative abundance of *ESR1* mRNA gradually declined to almost undetectable values ($P < 0.01$) within 6 h after $PGF_{2\alpha}$ treatment and then remained at low levels thereafter (Fig. 3).

Prior to treatment, the steady-state levels of *IL1B* mRNA were similar in CL of both luteal stages (Fig. 4). Following $PGF_{2\alpha}$ injection, the relative abundance of *IL1B* mRNA increased gradually ($P < 0.01$) and similarly during the first 3 h in both day 4 and day 9 CL (Fig. 4). On day 4 of pseudopregnancy, the luteal *IL1B* relative mRNA abundance peaked 2-fold ($P < 0.01$) above the basal level 3 h after $PGF_{2\alpha}$ challenge and thereafter gradually fell to pretreatment values. In day 9 CL, *IL1B* mRNA reached the peak level 6 h after the $PGF_{2\alpha}$ challenge, and then fell to pretreatment values (Fig. 4).

3.4. Gene and protein expression of TP53

The steady-state levels of *TP53* mRNA were comparable in CL explanted at both early and mid-luteal phases (Fig. 5, A and B). On day 4 of pseudopregnancy, the *TP53* mRNA levels gradually decreased ($P < 0.01$) during the 24 h after the treatment. On day 9 of pseudopregnancy, the *TP53* mRNA levels rose ($P < 0.01$) until 3 h after $PGF_{2\alpha}$ treatment and then gradually decreased to reach values lower ($P < 0.01$) than pretreatment values (Fig. 5, B).

Before $PGF_{2\alpha}$ challenge, TP53 protein was barely expressed in both day 4 and day 9 CL (Fig. 5, C and D). After $PGF_{2\alpha}$ treatment, an increase ($P < 0.01$) in the abundance of TP53 was observed in CL of both stages (Fig. 5, D). In day 4 CL, protein expression for TP53 increased ($P < 0.01$) within 1.5 h after $PGF_{2\alpha}$ injection to reach 30-fold higher values 3 h later and then gradually declined to levels 8-fold higher ($P < 0.01$) than pretreatment values (Fig. 5, D). In day 9 CL, TP53 protein concentrations gradually increased ($P < 0.01$) from 3 to 12 h after $PGF_{2\alpha}$ administration but fell ($P < 0.01$) to almost undetectable values 24 h later (Fig. 5, D).

3.5. Gene expression of BAX and BCL2L1

The steady-state levels of *BAX* transcript were similar in CL of both stages (Fig. 6, A and B). On day 4 of pseudopregnancy, the *BAX* mRNA concentrations were not affected by the treatment (Fig. 6, B). In day 9 CL, the expression for *BAX* mRNA remained at the same high concentrations for the first 3 h after $PGF_{2\alpha}$ administration and then decreased ($P < 0.01$) to half values thereafter (Fig. 6, B). Before treatment, the steady-state level of *BCL2L1* transcript was greater ($P < 0.01$) in day 4 than in day 9 CL (Fig. 6, C and D). On day 4 of pseudopregnancy, after $PGF_{2\alpha}$ injection, the *BCL2L1* mRNA concentrations remained the same for the next 24 h (Fig. 6, D). In day 9 CL, *BCL2L1* mRNA relative abundance decreased ($P < 0.01$) 6 h after $PGF_{2\alpha}$ administration and remained low ($P < 0.01$) thereafter (Fig. 6, D). The expression ratio of *BAX*/*BCL2L1* mRNAs in day

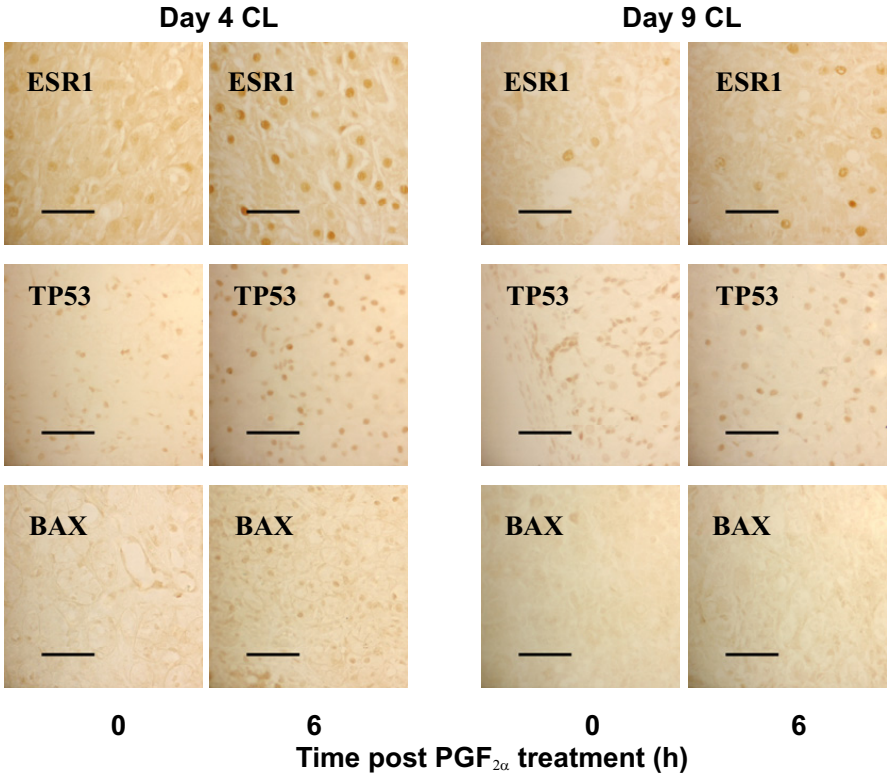

Fig. 2. Details of microphotographs of corpora lutea derived from the immunohistochemical analysis of ESR1, BAX, and TP53 in rabbit ovaries collected on days 4 and 9 of pseudopregnancy before (time 0) and 6 h after $PGF_{2\alpha}$ injection. Positive staining is shown as brown coloring. ESR1, TP53, and BAX show positive nuclear reaction of different intensity within luteal cells. In ESR1 microphotographs, bars = 10μm; in TP53 and BAX, bars = 40 μm.

4 CL was lower than in day 9 CL (0.61 ± 0.15 vs 1.23 ± 0.13, respectively, $P < 0.01$) and did not change following $PGF_{2\alpha}$ administration. In day 9 CL, the *BAX*/*BCL2L1* ratio increased 1.7-fold ($P < 0.01$) only 24 h after the $PGF_{2\alpha}$ challenge.

3.6. Protein expression of BAX and BCL2L1

Anti-BAX antibody detected an immunoblot protein doublet at approximately 21 kDa in CL of both luteal stages before and after $PGF_{2\alpha}$ treatment. BAX protein steady-state levels were 5-fold greater ($P < 0.01$) in day 4 than in day 9 CL (Fig. 7, A and B). In day 4 CL, BAX protein abundance decreased 4-fold ($P < 0.01$) 1.5 h after $PGF_{2\alpha}$ treatment and then remained at the same low concentrations thereafter, except for a peak 12 h later (Fig. 7, B). In day 9 CL, abundance of BAX protein remained fairly constant after $PGF_{2\alpha}$ administration at values similar to pretreatment values, except for a 5-fold increase ($P < 0.01$) 24 h later (Fig. 7B).

Before treatment, BCL2L1 protein was undetectable in both day 4 and day 9 CL (Fig. 7, C and D). In day 4 CL, immunoreactive bands for BCL2L1 were observed only 6, 12, and 24 h after $PGF_{2\alpha}$ injection, with a peak ($P < 0.01$) at 12 h (Fig. 7, C and D). In day 9 CL, BCL2L1 protein remained untraceable following $PGF_{2\alpha}$ challenge (Fig. 7, C and D).

3.7. Nitric oxide synthase enzymatic activity

The steady-state activity of total luteal NOS was comparable in both day 4 and day 9 CL (Fig. 8). For the first 3 h following $PGF_{2\alpha}$ challenge, NOS activity rose similarly almost 2-fold ($P < 0.01$) in CL of both luteal stages (Fig. 8). Thereafter, NOS activity declined ($P < 0.01$) to pretreatment values in day 4 CL, whereas it continued to rise ($P < 0.01$) in day 9 CL up to 6 h after $PGF_{2\alpha}$ injection, and then decreased ($P < 0.01$) to basal concentrations (Fig. 8).

4. Discussion

Corpora lutea regression via apoptotic pathways has been demonstrated in several species [19–21], but the actual factors triggered by $PGF_{2\alpha}$ remain to be identified. On the other hand, the molecular mechanisms that protect the CL from the onset of luteolysis in the early stages of luteal development are poorly known. In fact, one of the most intriguing facets of luteal physiology

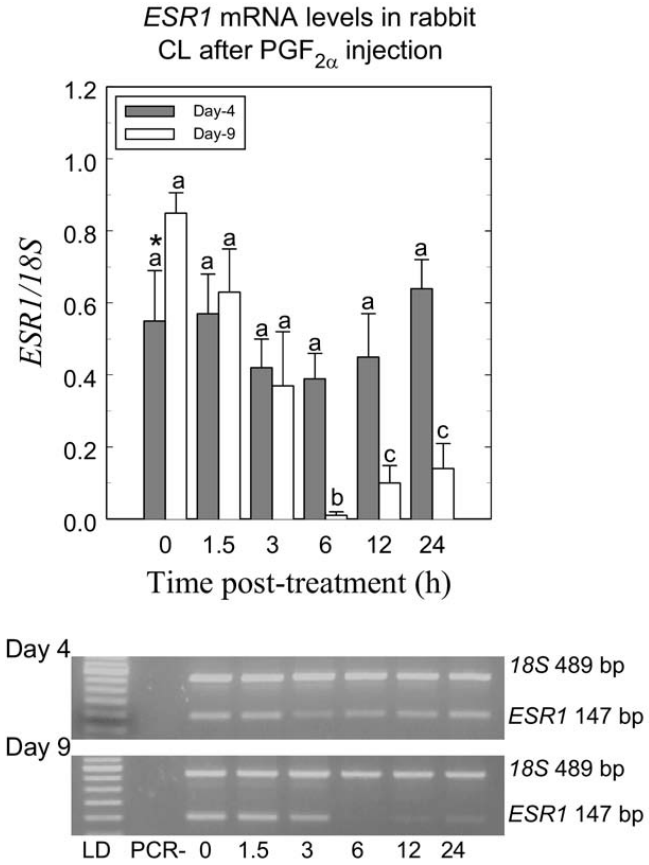

Fig. 3. *ESR1* mRNA relative abundance in rabbit CL harvested just before and at different time intervals after $PGF_{2\alpha}$ injection on day 4 or day 9 of pseudopregnancy. The lower panels show representative photographs of typical 2% agarose ethidium bromide-stained gels, showing the presence of the expected bp products yielded after reverse transcriptase polymerase chain reaction (RT-PCR) using primers for target *ESR1* (147 bp) and *18S* (489 bp). Lane LD is the kb DNA marker, lane PCR-represents a negative control of non-reverse-transcribed RNA submitted to PCR amplification, whereas the other lanes identify the corresponding hours after $PGF_{2\alpha}$ injection. For each luteal stage, the values (means ± SD), derived from densitometric analyses of *ESR1* reported in arbitrary units relative to *18S* expression, combine the results from 3 different rabbits for each time point. Within each luteal stage, different letters above bars indicate a significantly different value ($P < 0.01$). An asterisk points to a significant difference ($P < 0.01$) of the pretreatment values (time 0) between luteal stages.

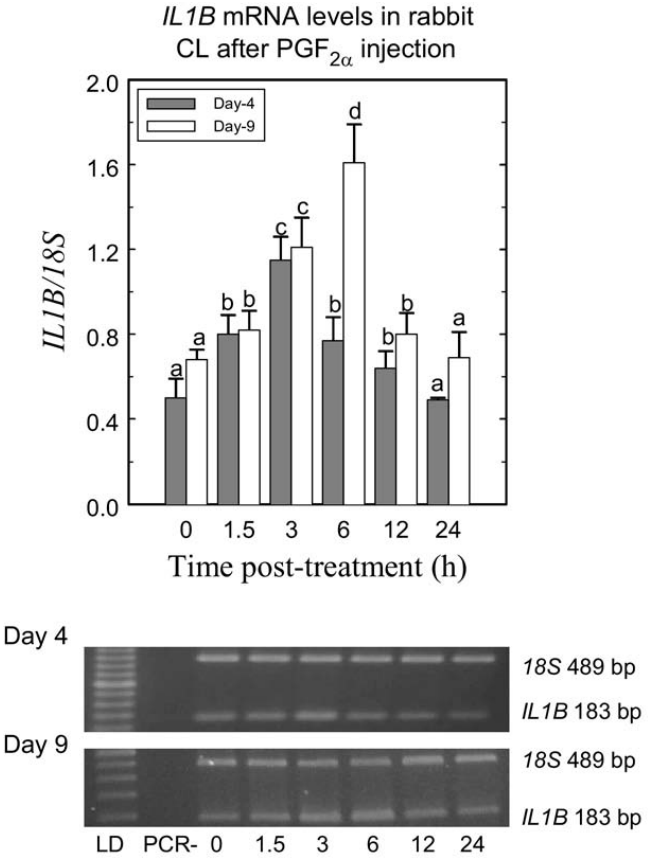

Fig. 4. *IL1B* mRNA relative abundance in rabbit corpora lutea harvested just before and at different time intervals after $PGF_{2\alpha}$ injection on day 4 or day 9 of pseudopregnancy. The lower panels show representative photographs of typical 2% agarose ethidium bromide-stained gels, showing the presence of the expected bp products yielded after reverse transcriptase polymerase chain reaction using primers for target *IL1B* (183 bp) and *18S* (489 bp). Lane LD is the kb DNA marker, lane PCR-represents a negative control of non-reverse-transcribed RNA submitted to PCR amplification, whereas the other lanes identify the corresponding hours after $PGF_{2\alpha}$ injection. For each luteal stage, the values (means ± SD), derived from densitometric analyses of *IL1B* reported in arbitrary units relative to *18S* expression, combine the results from 3 different rabbits for each time point. Within each luteal stage, different letters above bars indicate a significantly different value ($P < 0.01$).

concerns the understanding of what cellular and molecular mechanisms confer CL the sensitivity to the luteolytic action of $PGF_{2\alpha}$ at a precise stage of their development. As in other species [8,9], rabbit CL are not completely refractory to $PGF_{2\alpha}$ in the early stages of development during pseudopregnancy, and several changes occur at molecular and genetic levels, although luteal steroidogenesis is not impaired [6,7]. In this study, through RT-PCR, WB, and IHC, we provide further evidence that exogenous $PGF_{2\alpha}$ differentially modulates luteal expression for *ESR1 IL1B TP53*, *BAX*, and *BCL2L1* transcripts as well as that for TP53, BAX, and BCL2L1 proteins, depending on luteal stage. These differential expression responses to $PGF_{2\alpha}$ at the gene and protein level are consistent with CL changes of key factors that may drive intraluteal cell molecular networks toward acquisition of luteolytic capacity and apoptosis.

Growing evidence suggests that, through genomic regulations mediated by estrogen receptor, estradiol-17β exerts both luteotrophic and luteolytic actions depending on the species [22]. In the ovary of rabbits, ESR1 is the dominant isoform and is predominantly

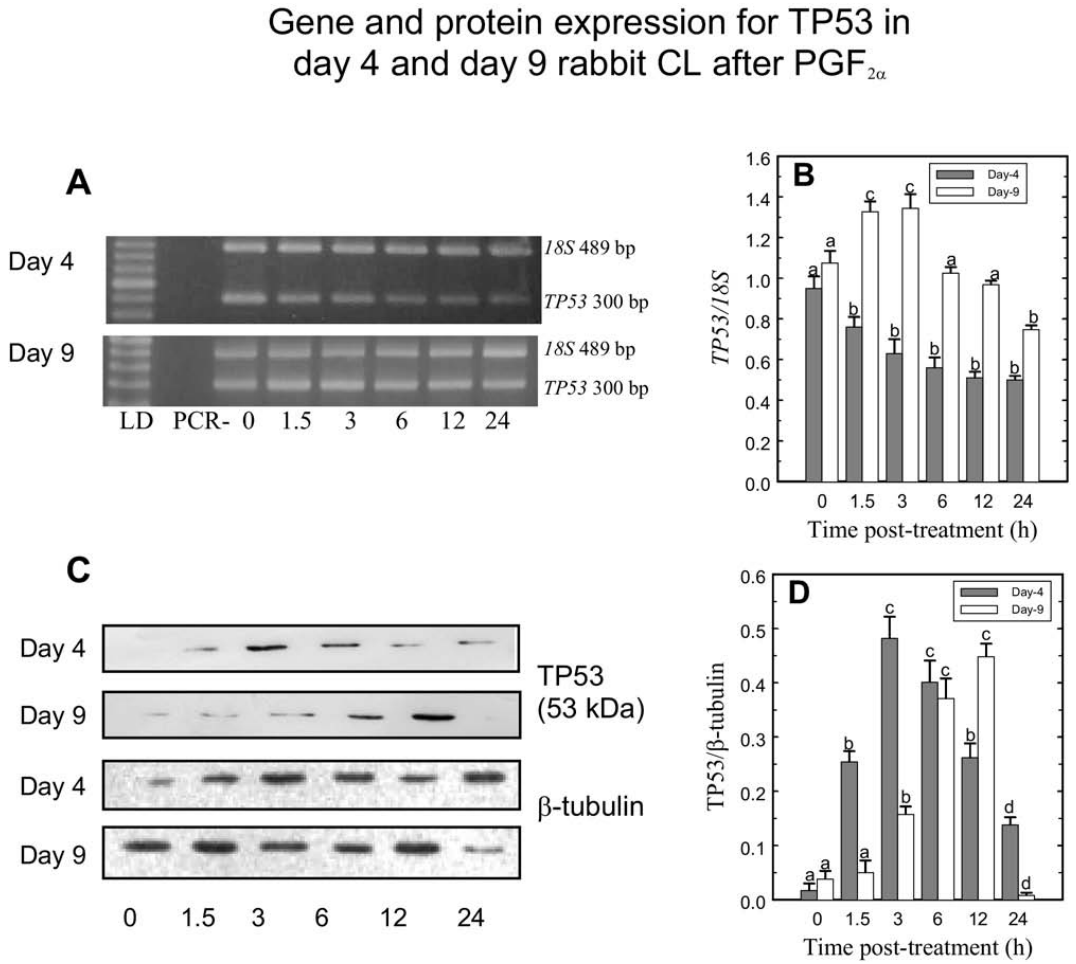

Fig. 5. Relative abundances of *TP53* mRNA and protein in rabbit corpora lutea harvested just before and at different time intervals after $PGF_{2\alpha}$ injection on day 4 or day 9 of pseudopregnancy. In A, representative photographs of typical 2% agarose ethidium bromide-stained gels, showing the presence of the expected bp products yielded after reverse transcriptase polymerase chain reaction (RT-PCR) using primers for target *TP53* (300 bp) and *18S* (489 bp). Lane LD is the kb DNA marker, lane PCR-represents a negative control of non-reverse-transcribed RNA submitted to PCR amplification, whereas the other lanes identify the corresponding hours after $PGF_{2\alpha}$ injection. In B, data (means ± SD) derived from densitometric analyses of *TP53* in CL reported in arbitrary units relative to *18S* expression. In C, representative immunoblots of TP53 and β-tubulin; in D, densitometric analyses of the blots reported in arbitrary units relative to β-tubulin. For each luteal stage, the values for gene and protein expressions combine the results from 3 different rabbits for each time point. Within each luteal stage, different letters above bars indicate a significantly different value ($P < 0.01$).

associated with the cytosolic compartment [23]. The regulation of *ESR1* expression has been investigated in numerous species, including the rabbit, but to the best of our knowledge, no study has been conducted on rabbit CL during spontaneous or $PGF_{2\alpha}$-induced luteolysis. A clear difference in the steady-state levels for *ESR1* transcript emerged between the early and mid-luteal stages, with day 4 lower than day 9 CL. However, although its relative mRNA abundance remained unaffected following $PGF_{2\alpha}$ challenge in day 4 CL, *ESR1* mRNA was greatly down-regulated in day 9 CL as early as 6 h after $PGF_{2\alpha}$ injection. Interestingly, the decrease in *ESR1* transcript coincided with progesterone decline, which occurred 6 h after $PGF_{2\alpha}$ injection in luteal tissue of mid-pseudopregnancy and approximately 8 h later in peripheral blood [12]. Previous studies indicated that the loss of steroidogenesis in the rabbit CL is associated with the concomitant loss of luteal estrogen receptor, and that there is a relationship between luteal estrogen receptor content and estradiol-stimulated progesterone synthesis [24]. Based on their morphological appearance, most of the ESR1 immunoreactive cells were steroidogenic, with round nuclei and vacuolized cytoplasms. However, the elongated aspect of some ESR1-positive nuclei suggests that other types of luteal cells may also express ESR1.

Current evidence suggests that luteolysis may be an immune-mediated event, and resident immune cells are now recognized as key modulators of the CL functional lifespan by acting on nearby luteal, endothelial, stro-

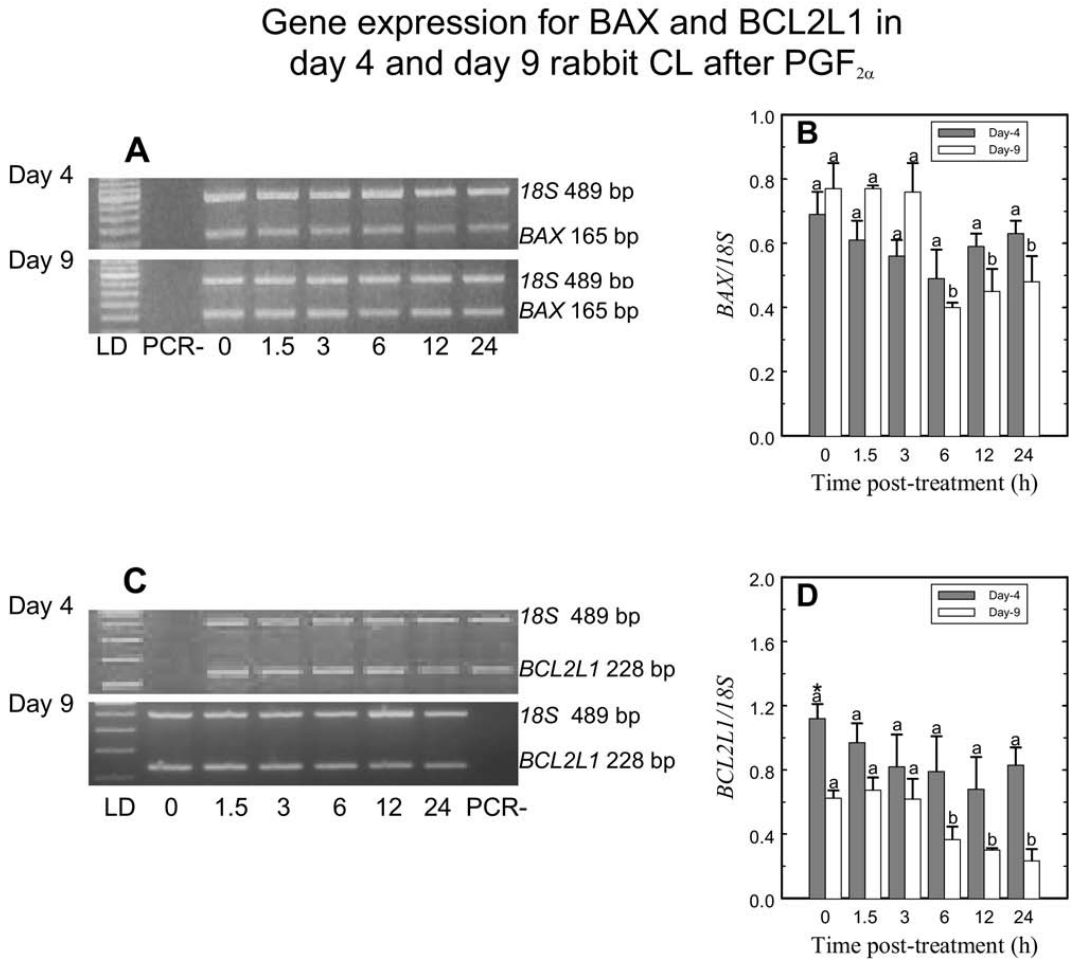

Fig. 6. Relative abundances of *BAX* and *BCL2L1* mRNAs in rabbit corpora lutea (CL) harvested just before and at different time intervals after $PGF_{2\alpha}$ injection on day 4 or day 9 of pseudopregnancy. In A and C, representative photographs of typical 2% agarose ethidium bromide stained gels, showing the presence of the expected bp products yielded after reverse transcriptase polymerase chain reaction (RT-PCR) using primers for target *BAX* (165 bp), *BCL2L1* (228 bp), and *18S* (489 bp). Lane LD is the kilobase DNA marker, lane PCR-represents a negative control of non-reverse-transcribed RNA submitted to PCR amplification, whereas the other lanes identify the corresponding hours after $PGF_{2\alpha}$ injection. In B and D, data derived from densitometric analyses of *BAX* and *BCL2L1*, respectively, in CL reported in arbitrary units relative to *18S* expression. For each luteal stage, the values for gene expressions (means ± SD) combine the results from 3 different rabbits for each time point. Within each luteal stage, different letters above bars indicate a significantly different value ($P < 0.01$). An asterisk points to a significant difference ($P < 0.01$) of the pretreatment values (time 0) between luteal stages.

mal, and immune cells through a large array of cytokines [12,25,26]. Among these, IL1 has been identified in the ovary of several species, including the rabbit [27], where it plays a role in follicular development, ovulation, and steroidogenesis [28]. Although it is evident that IL1B greatly influences ovarian and CL physiology, there have been controversial results concerning its specific mechanism of action. In the present study, following $PGF_{2\alpha}$ challenge, luteal *IL1B* mRNA was up-regulated within 3 h on both day 4 and day 9 of pseudopregnancy, but thereafter, the dynamic expression pattern differed depending on luteal stage. The reason for this differential response might depend on changes in CL cell composition and in intraluteal endocrine milieu. In fact, although the monocyte/macrophage system, a normal but very modest component of the developing rabbit CL [29,26], is the primary source of *IL1B*, this cytokine is also released by other cells of the ovary, including fibroblasts, endothelial, luteal [30], granulose, and theca cells [28]. Increasing numbers of immune cells have been reported in rabbits during spontaneous luteal regression [27,11]. Thus, the increased gene expression for luteal *IL1B* after $PGF_{2\alpha}$ administration detected at day 9 of pseudopregnancy may be related to the influx of macrophages at this time, as observed in bovines [31].

Interleukin-1β exerts a wide array of actions in the ovary [32]; it decreases progesterone secretion, increases prostaglandin synthesis, induces $PGF_{2\alpha}$ receptor expression, inhibits cyclooxygenase-2 (*COX2)*

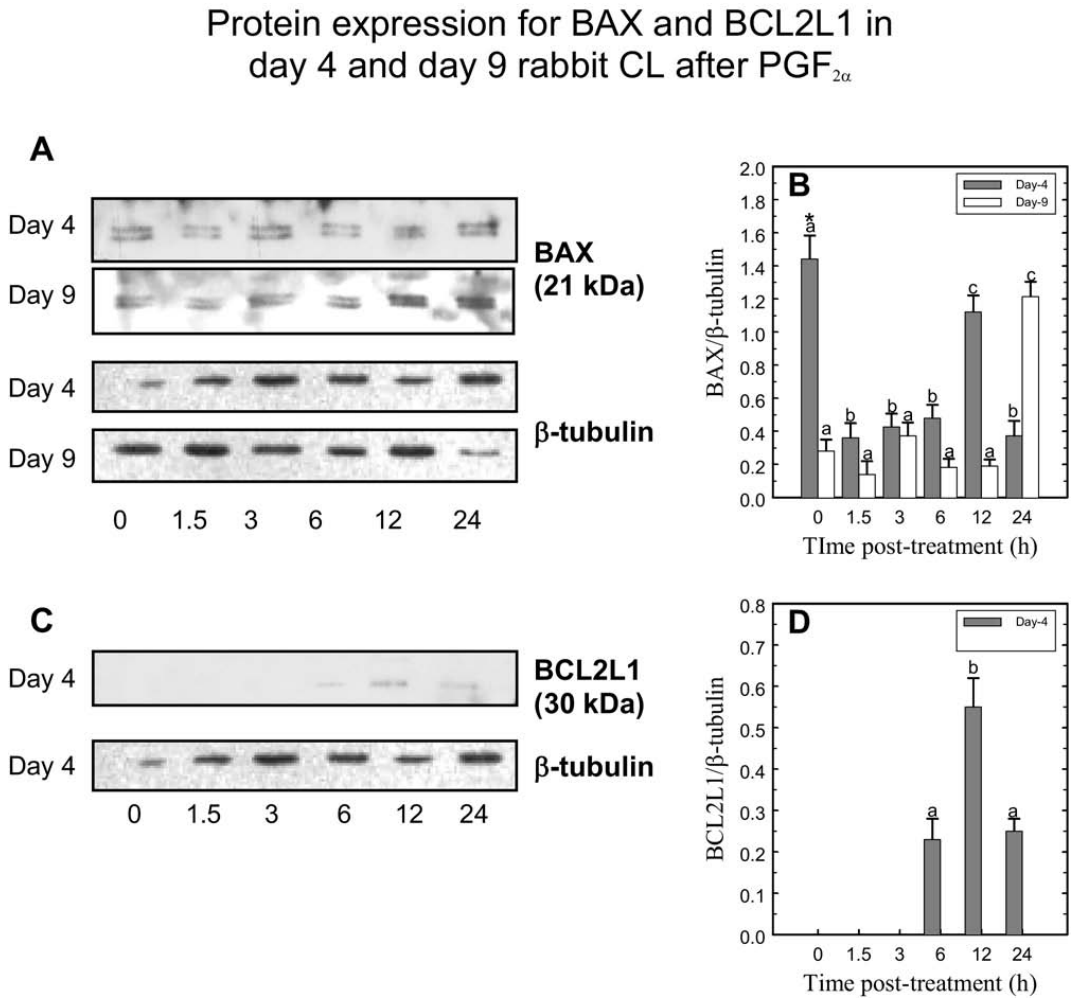

Fig. 7. Relative abundances of BAX and BCL2L1 proteins in rabbit corpora lutea harvested just before and at different time intervals after $PGF_{2\alpha}$ injection on day 4 or day 9 of pseudopregnancy. In A and C, representative immunoblots of BAX and BCL2L1, respectively; in B and D densitometric analyses of the BAX and BCL2L1 blots, respectively, reported in arbitrary units relative to β-tubulin. Doublet bands at approximately 21 kDa were detected for BAX (A). For each luteal stage, the values (means ± SD) for protein expression combine the results from 3 different rabbits for each time point. Within each luteal stage, different letters above bars indicate a significantly different value ($P < 0.01$). An asterisk points to a significant difference ($P < 0.01$) of the pretreatment values (time 0) between luteal stages.

mRNA degradation [33], and enhances NO production, activating constitutive and/or inducible NOS [30]. Recently, we found that $PGF_{2\alpha}$ injection caused a marked up-regulation of *COX2* expression and activity, as well as increased $PGF_{2\alpha}$ release only in day 9 CL that had acquired a luteolytic capacity [7]. Therefore, given the present and previous data, the overexpression of IL1B mRNA soon after exogenous $PGF_{2\alpha}$ administration suggests, although indirectly, that this cytokine may be involved in enhancing intraluteal $PGF_{2\alpha}$ synthetic pathways by the up-regulation of luteal NOS and *COX2* activities. Thus, these findings suggest that IL1B plays a pivotal role in promoting the functional regression of CL that have gained luteolytic capability.

Following $PGF_{2\alpha}$ challenge, total luteal NOS activity was markedly up-regulated within 1.5 h on both day 4 and day 9 of pseudopregnancy. However, the dynamic pattern of NOS activity subsequently differed between the early and mid-luteal stages. In fact, in early CL, NOS activity decreased to pretreatment values, whereas in mature CL, it peaked 6 h after $PGF_{2\alpha}$ injection to sharply decrease to basal levels in the following hours. It is now evident that NO has pleiotropic actions, as it is involved in immune response as well as in cell differentiation and apoptosis in several systems in which it modulates key functions in many physiological and pathological processes [34]. *In vitro* and *in vivo* data have shown that within the ovary, NO controls ovulation and regulates luteal steroidogenesis as well as luteal regression by targeting both nitration and oxidation of specific proteins [35]. Nitric oxide exerts both anti- and pro-apoptotic effects in many

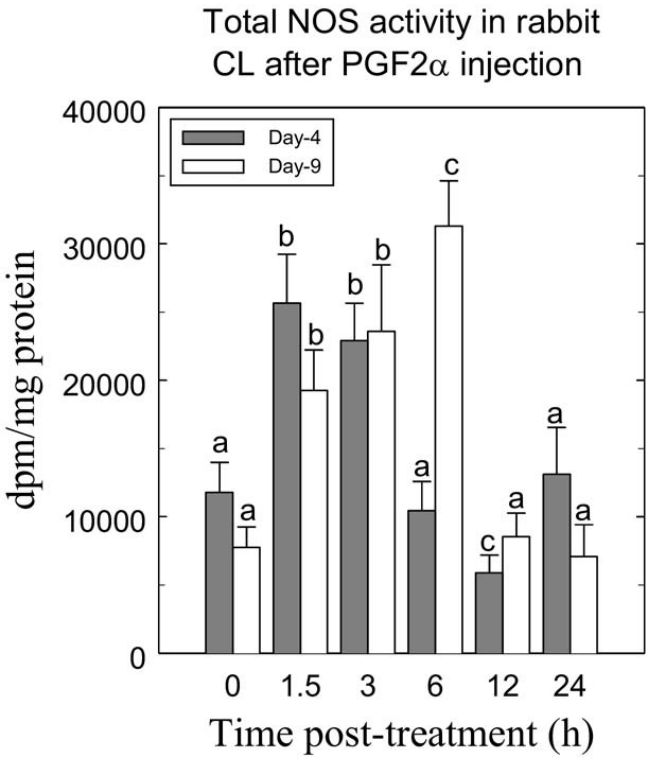

Fig. 8. Total NOS activity in rabbit corpora lutea explanted just before and at different time intervals after $PGF_{2\alpha}$ injection on day 4 or day 9 of pseudopregnancy. For each luteal stage, the values combine the results from 3 different rabbits for each time point. Within each luteal stage, different letters above bars indicate a significantly different value ($P < 0.01$).

biological systems. The anti-apoptotic effects of NO include inhibition of caspases, increase of heat shock proteins (HSPs) and BCL2, and nitration of TP53 and activation of Akt/PKB pathways, which induces cytoprotective gene expression through NF-kB activation [36]. On the other hand, nitrosative stress can promote apoptosis through the activation of mitochondrial pathways, such as the release of cytochrome C and endonuclease G, as well as the inhibition of NF-kB, decreased BCL2 expression, and increased TP53 expression [37].

Total NOS activity was much higher in rabbit CL explanted on day 9 than on day 4 of pseudopregnancy and cultured in vitro after incubation with $PGF_{2\alpha}$ [3]. In bovine luteal cells, reactive oxygen species (ROS) were found to modulate the activation of the signaling pathway for luteal-cell apoptosis by up-regulating *COX2*, *TP53*, and *BAX* mRNA expression [38]. This regulatory action of ROS, however, likely also occurs in vivo during spontaneous CL regression at the end of the estrous cycle or following $PGF_{2\alpha}$-induced luteolysis. In fact, one of the primary responses to cellular damage, such as that elicited by ROS [39], is the stabilization and nuclear translocation of the anti-oncogenic transcription factor *TP53* [40].

Among several functions, the transcriptional factor TP53 acts as a tumor suppressor by causing growth arrest or apoptosis in response to a variety of cellular stresses [41]. The TP53 protein interacts with at least 6 members of the BCL2 family, whose gene is alternatively processed to yield both negative ("long" isoform, death suppressor, BCLXL) and positive ("short" isoform, death inducer, BCLXS) regulators of the cell death pathway, by inhibiting the anti-apoptotic BCLXL member and activating the pro-apoptotic BAX [42]. Interestingly, in the present study, the steady-state levels for the *TP53* pro-apoptotic and *BAX* gene transcripts were comparable in both day 4 and day 9 CL, whereas those for the anti-apoptotic *BCL2L1* gene showed a different trend and were higher in day 4 than in day 9 CL. Thus, the *BAX*/*BCL2L1* mRNA ratio, an index used for discerning the susceptibility of a cell system to apoptotic signals, was lower in day 4 than in day 9 CL. However, when the expression of proteins was evaluated by WB, the level of TP53 was very low at both luteal stages, whereas the abundance of BAX was higher in day 4 than in day 9 CL and that for BCL2L1 was undetectable in both young and mature CL.

Independently of luteal stage, using anti-BAX antibody, we consistently observed an immunoblot doublet both before and after $PGF_{2\alpha}$ treatment. Similar findings have been reported in rabbits [43] and in rats [44]. Using the IHC technique, positive reaction for TP53 and BAX, although at different levels of intensity, was found in luteal cells of CL obtained from both early and mid-luteal phases before $PGF_{2\alpha}$ administration. By contrast, immunohistochemical staining for BCL2L1 was absent in CL and, within the ovary, was observed only in the oocytes of primary follicles, suggesting that this member of the BCL2 family controls its survival from apoptotic stimuli.

Our data confirm that TP53 and BAX proteins are constitutively expressed in rabbit CL at different stages of development, similarly to what has been found in CL of other species [45–47]. Although the role of TP53, BAX, and BCL2L1 in regulating the luteolytic cascade is still controversial, these findings suggest that day 4 and day 9 CL are both intrinsically susceptible to the apoptotic process. It remains to be explained what factors, either directly or indirectly, cause this imbalance between pro- and anti-apoptotic gene and protein expressions on CL at different stages of development. However, the finding that placental-derived factors promoted luteal cell survival in pregnant rabbits [20] indirectly suggests that endocrine-mediated mechanisms

may regulate the expression of these genes. In addition, progesterone is also known to exert a protective action on luteal cell survival and to oppose functional regression of CL [48]. Therefore, intraluteal factors acting locally, in a paracrine and/or autocrine way, may also be involved in modulating the expression of pro- and anti-apoptotic genes. Intriguingly, however, BCL2L1 was not expressed at the protein level in CL of pseudopregnant rabbits, suggesting that species-related differences may exist. In fact, although the *BCL2L1* gene is not required for CL establishment and maintenance, BCL2L1 protein was identified in granulosa and luteal cells of the mouse ovary [49].

On day 4 of pseudopregnancy, in $PGF_{2\alpha}$-uncompetent CL, *TP53* transcript declined following administration of a luteolytic dose of the synthetic prostaglandin, whereas *BAX* and *BCL2L1* mRNAs remained almost unaffected and their ratio consistently low. However, the abundance of TP53 protein markedly increased, whereas that of BAX decreased within 1.5 h after $PGF_{2\alpha}$ challenge. A similar trend was maintained during the next several h, although at different levels.

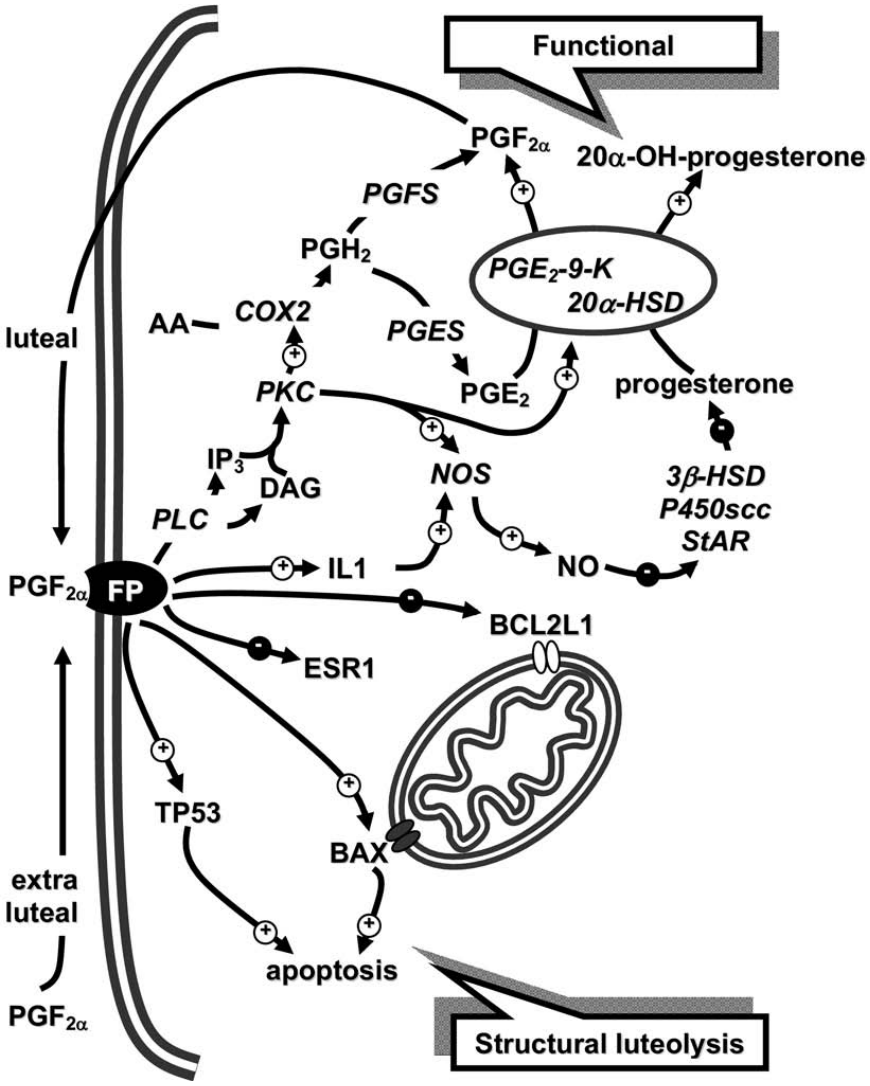

Fig. 9. Simplified model showing the intracellular signaling luteolytic pathways activated by $PGF_{2\alpha}$ in a rabbit luteal cell at day 9 of pseudopregnancy. 3β-HSD: 3β-hydroxysteroid dehydrogenase; 20α-HSD: 20α-hydroxysteroid dehydrogenase; AA: arachidonic acid; BCL2L1**:** B-cell CLL/lymphoma 2 (BCL2) -like 1 (BCL2L1)**;** BAX: BCL2-associated X protein, COX2: cyclooxygenase 2; DAG: diacylglycerol; ESR1: estrogen receptor, subtype-1; IL1B: interleukin-1beta; IP3: inositol triphosphate; FP: $PGF_{2\alpha}$ receptor; NO: nitric oxide; NOS: nitric oxide synthase; P450scc: cytochrome P450 side-chain cleavege; PGE_2, prostaglandin E_2; PGE_2-9-K: PGE_2-9-ketoreductase; PGES: prostaglandin E_2 synthase; $PGF_{2\alpha}$: prostaglandin $F_{2\alpha}$; PGFS: prostaglandin $F_{2\alpha}$ synthase; PGH_2, prostaglandin H_2; PKC: protein kinase C; PLC: phospholipase C; StAR: steroidogenic acute regulatory protein: TP53: tumor protein p53. PGE_2-9-K and 20α-HSD are joined as they represent a single enzyme with 2 different activities. In this working model, enzymes are in italics.

Interestingly, BCL2L1, which was undetectable prior to treatment, was expressed 6 h after $PGF_{2\alpha}$ administration. Positive bands for BCL2L1 were also clearly observed 12 and 24 h later, which correlated with the resistance of early luteal phase CL to the luteolytic action of $PGF_{2\alpha}$. By contrast, in $PGF_{2\alpha}$-competent CL at day 9 of pseudopregnancy, the *TP53* gene was initially up-regulated within 3 h after $PGF_{2\alpha}$ administration, but then returned to pretreatment values during the course of functional luteolysis. *BAX* mRNA was markedly down-regulated 6 h after $PGF_{2\alpha}$ administration, and a similar finding was observed for *BCL2L1*. As a consequence, the ratio of relative levels of mRNA encoding *BAX* and *BCL2L1*, fairly constant during $PGF_{2\alpha}$-induced luteolysis, increased 24 h after treatment. By contrast, neither *BCL2L1* nor *TP53* mRNA levels changed in functional versus regressed bovine CL [45]. Similarly, these 2 gene apoptotic markers remained unaffected in rat CL during spontaneous regression [50].

In the present study, both TP53 and BAX proteins increased in mid-luteal stage CL following $PGF_{2\alpha}$ challenge, although at different time intervals and with different rates, but the protein product of TP53 became undetectable 24 h after treatment. By contrast, no signal for BCL2L1 was appreciable by WB analysis throughout $PGF_{2\alpha}$-induced luteolysis and by IHC at the time points investigated. Western blot analysis revealed a gradual reduction in TP53 protein in the rat CL during luteal regression [50]. The apoptosis-regulating protein BAX was expressed constantly in the human CL throughout the luteal phase [51]. Injection of $PGF_{2\alpha}$ triggered an increased ratio of BAX to BCL2 in CL of bison cows as early as 4 h post-treatment that remained elevated until 18 h [46]. The lack of temporal and quantitative coincidence between transcript and protein expressions observed in our study either before or after $PGF_{2\alpha}$ treatment provides unequivocal proof that dynamic and complex post-transcriptional processes regulate luteal apoptotic pathways. Part of the explanation, however, may reside in the continuous remodeling that characterizes CL development in the rabbit involving both luteal and nonluteal cells [52].

Our findings clearly suggest that the apoptotic system controlled by these genes is actively involved in an opposite way, either inhibited or enhanced depending on luteal stage. Taken together, these contrasting findings suggest that the mechanism leading to apoptosis in the mammalian CL may differ among species. However, as a note of caution, it should be borne in mind that spontaneous and $PGF_{2\alpha}$-induced luteal regression are not fully superimposable processes.

In conclusion, through the dynamic changes of key genes that encode proteins directly involved in the control of the apoptotic mechanism, we have demonstrated for the first time in rabbits that during $PGF_{2\alpha}$-evoked luteolysis in CL that have acquired a luteolytic capacity, the concurrent up-regulation of luteal *IL1B* and *TP53* gene transcripts and NOS activity precedes the down-regulation of *ESR1* and *BCL2L1* genes (Fig. 9). The regression effect on CL after $PGF_{2\alpha}$ treatment appears to be a result of distinct processes that involve the steroidogenic pathway, as shown by *ESR1* down-regulation, as well as apoptotic signaling, as shown by the dynamic changes of TP53 and BCL2L1 proteins and gene transcripts. Given that NO is involved in immune response, cell differentiation, and apoptosis, the distinct phases of activation/modulation of the single genes involved in the apoptotic process are consistent with the regulatory role of ROS owing to the action of the $PGF_{2\alpha}$.

Acknowledgments

This work was supported by a grant from the Ministero dell'Istruzione, dell'Università e della Ricerca (Contract n. 2005074002_003). The authors gratefully acknowledge the revision of the English text by Sheila Beatty. The authors wish to thank Mrs. G. Mancini for her excellent technical assistance.

References

[1] Lytton FDC, Poyser NL. Concentrations of $PGF_{2\alpha}$ and PGE-2 in the uterine venous blood of rabbits during pseudopregnancy and pregnancy. J Reprod Fertil. 1982;64:421–429.

[2] Webb R, Woad KJ, Armstrong DG. Corpus luteum (CL) function: local control mechanism. Domest Anim Endocrinol. 2002; 23:277–285.

[3] Boiti C, Zerani M, Zampini D, Gobbetti A. Nitric oxide synthase activity and progesterone release by isolated corpora lutea of rabbits in early- and mid-luteal phase of pseudopregnancy are differently modulated by prostaglandin E-2 and prostaglandin F-2α via adenylate cyclase and phospholipase C. J Endocrinol. 2000;164:179–186.

[4] Boiti C, Guelfi G, Zampini D, Brecchia G, Gobbetti A, Zerani M. Regulation of nitric-oxide synthase isoforms and role of nitric oxide during prostaglandin F2α-induced luteolysis in rabbits. Reproduction. 2003;125:807–816.

[5] Boiti C, Guelfi G, Brecchia G, Dall'Aglio C, Ceccarelli P, Maranesi M, Mariottini C, Zampini D, Gobbetti A, Zerani M. Role of endothelin-1 system in the luteolytic process of pseudopregnant rabbits. Endocrinology. 2005;146:1293–1300.

[6] Boiti C, Maranesi M, Dall'Aglio C, Pascucci L, Brecchia G, Gobbetti A, Zerani M. Vasoactive peptides in the luteolytic

process activated by PGF2alpha in pseudopregnant rabbits at different luteal stages. Biol Reprod. 2007;77:156–164.

[7] Zerani M, Dall'Aglio C, Maranesi M, Gobbetti A, Brecchia G, Mercati F, Boiti C. Intraluteal regulation of prostaglandin F2 alpha-induced prostaglandin biosynthesis in pseudopregnant rabbits. Reproduction. 2007;133:1005–1016.

[8] Diaz FJ, Wiltbank MC. Acquisition of luteolytic capacity involves differential regulation by prostaglandin F2α of genes involved in progesterone biosynthesis in the porcine corpus luteum. Domest Anim Endocrinol. 2005;28:172–189.

[9] Tsai SJ, Wiltbank MC. Prostaglandin F2α regulates distinct physiological changes in early and mid-cycle bovine corpora lutea. Biol Reprod. 1998;58:346–352.

[10] Boiti C, Canali C, Zerani M, Gobbetti A. Changes in refractoriness of rabbit corpora lutea to a prostaglandin F2α analogue, alfaprostol, during pseudopregnancy. Prostaglandins. 1998;56: 255–264.

[11] Krusche CA, Vloet TD, Herrier A, Black S, Beier HM. Functional and structural regression of the rabbit corpus luteum is associated with altered luteal immune cell phenotypes and cytokine expression patterns. Histochem Cell Biol. 2002;118: 479–489.

[12] Boiti C, Guelfi G, Zerani M, Zampini D, Brecchia G, Gobbetti A. Expression patterns of cytokines, p53, and nitric oxide synthase isoenzymes in corpora lutea of pseudopregnant rabbits during spontaneous luteolysis. Reproduction. 2004;127:229–238.

[13] Del Vecchio RP, Sutherland WD. Prostaglandin and progesterone production by bovine luteal cells incubated in the presence or absence of the accessory cells of the corpus luteum and treated with interleukin-1beta, indomethacin and luteinizing hormone. Reprod Fertil Dev. 1997;9:651–658.

[14] Goodman SB, Kugu K, Chen SH, Preutthipan S, Tilly KI, Tilly JL, Dharmarajan AM. Estradiol-mediated suppression of apoptosis in the rabbit corpus luteum with a shift in expression of Bcl-2 family members favoring cellular survival. Biol Reprod. 1998;59:820–827.

[15] Leon L, Jeannin JF, Bettaieb A. Post-translational modifications induced by nitric oxide (NO): implication in cancer cells apoptosis. Nitric Oxide. 2008;19:77–83.

[16] Preutthipan S, Chen SH, Tilly JL, Kugu K, Lareu, RR, Dharmarajan AM. Inhibition of nitric oxide synthesis potentiates apoptosis in the rabbit corpus luteum. Reprod Biomed Online. 2004;9:264–270.

[17] Dall'Aglio C, Ceccarelli P, Pascucci L, Brecchia G, Boiti C. Receptors for leptin and estrogen in the subcommissural organ of rabbits are differentially modulated by fasting. Brain Res. 2006;1124:62–69.

[18] Zerani M, Boiti C, Zampini D, Brecchia G, Dall'Aglio C, Ceccarelli P, Gobbetti A. Ob receptor in rabbit ovary and leptin in vitro regulation of corpora lutea. J Endocrinol. 2004;183: 279–288.

[19] Sugino N, Okuda K. Species-related differences in the mechanism of apoptosis during structural luteolysis. J Reprod Dev. 2007;53:977–986.

[20] Dharmarajan AM, Goodman SB, Atiya N, Parkinson SP, Lareu RR, Tilly KI, Tilly JL. Role of apoptosis in functional luteolysis in the pregnant rabbit corpus luteum: evidence of a role for placental-derived factors in promoting luteal cell survival. Apoptosis. 2004;9:807–814.

[21] Nicosia SV, Diaz J, Nicosia RF, Saunders BO, Muro-Cacho C. Cell proliferation and apoptosis during development and aging of the rabbit corpus luteum. Ann Clin Lab Sci. 1995;25: 143–157.

[22] Schams D, Berisha B. Steroids as local regulators of ovarian activity in domestic animals. Domest Anim Endocrinol. 2002; 23:53–65.

[23] Monje P, Boland R. Subcellular distribution of native estrogen receptor α and β isoforms in rabbit uterus and ovary. J Cell Biochem. 2001;82:467–479.

[24] Yuh KC, Keyes PL. Relationships between estrogen receptor and estradiol-stimulated progesterone synthesis in the rabbit corpus luteum. Biol Reprod. 1982;27:1049–1054.

[25] Adashi EY. The potential relevance of cytokines to ovarian physiology: the emerging role of resident ovarian cells of the white blood cell series. Endocrinol Rev. 1990;11:454–464.

[26] Bagavandoss P, Wiggins RC, Kunkel SL, Remick DG, Keyes PL. Tumor necrosis factor production and accumulation of inflammatory cells in the corpus luteum of pseudopregnancy and pregnancy in rabbits. Biol Reprod. 1990;42:367–376.

[27] Takehara Y, Dharmarajan AM, Kaufman G, Wallach EE. Effect of interleukin 1β on ovulation in the in vitro perfused rabbit ovary. Endocrinology. 1994;134:1788–1793.

[28] Bréard E, Delarue B, Benhaïm A, Féral C, Leymarie P. Inhibition by gonadotropins of interleukin-1 production by rabbit granulosa and theca cells: effects on gonadotropin-induced progesterone production. Eur J Endocrinol. 1998;138:328–336.

[29] Koering MJ. Luteolysis in normal and prostaglandin F2α-treated pseudopregnant rabbits. J Reprod Fertil. 1974;40:259–267.

[30] Estevez A, Tognetti T, Rearte B, Sander V, Motta AB. Interleukin1-beta in the functional luteolysis. Relationship with the nitric oxide system. Prostaglandins Leukot Essent Fatty Acids. 2002;67:411–417.

[31] Townson DH, O'Connor CL, Pru JK. Expression of monocyte chemoattractant protein-1 and distribution of immune cell populations in the bovine corpus luteum throughout the estrous cycle. Biol Reprod. 2002;66:361–366.

[32] Gérard N, Caillaud M, Martoriati A, Goudet G, Lalmanach AC. The interleukin-1 system and female reproduction. J Endocrinol. 2004;180:203–212.

[33] Narko K, Ritvos O, Ristmaki A. Induction of cyclooxygenase-2 and prostaglandin F2α receptor expression by interleukin-1β in cultured human granulose-luteal cells. Endocrinology. 1997; 138:3638–3644.

[34] Ignarro LJ. Physiology and pathophysiology of nitric oxide. Kidney Int Suppl. 1996;55:S2–5.

[35] Motta AB, Estevez A, Franchi A, Perez-Martinez S, Farina M, Ribeiro ML, Lasserre A, Gimeno MF. Regulation of lipid peroxidation by nitric oxide and $PGF_{2\alpha}$ during luteal regression in rats. Reproduction. 2001;121:631–637.

[36] Cobbs CS, Samanta M, Harkins LE, Gillespie GY, Merrick BA, MacMillan-Crow LA. Evidence for peroxynitrite-mediated modifications to p53 in human gliomas: possible functional consequences. Arch Biochem Biophys. 2001;394:167–172.

[37] Taylor BS, Kim YM, Wang Q, Shapiro RA, Billiar TR, Geller D. Nitric oxide down-regulates hepatocyte-inducible nitric oxide synthase gene expression. Arch Surg. 1997;132:1177–1183.

[38] Nakamura T, Sakamoto K. Reactive oxygen species up-regulates cyclooxygenase-2, p53, and Bax mRNA expression in bovine luteal cells. Biochem Biophys Res Commun. 2001;284: 203–201.

[39] Yu BP. Cellular defenses against damage from reactive oxygen species. Physiol Rev. 1994;74:139–162.

[40] Kastan MB, Onyekwere O, Sidransky D, Vogelstein B, Craig RW. Participation of p53 protein in the cellular response to DNA damage. Cancer Res. 1991;51:6304–6311.

[41] Liebermann DA, Hoffman B, Vesely D. p53 induced growth arrest versus apoptosis and its modulation by survival cytokines. Cell Cycle. 2007;6:166–170.

[42] Sot B, Freund SM, Fersht AR. Comparative biophysical characterization of p53 with the pro-apoptotic BAK and the anti-apoptotic BCL-xL. J Biol Chem. 2007;282:29193–29200.

[43] Lazou A, Iliodromitis EK, Cieslak D, Voskarides K, Mousikos S, Bofilis E, Kremastinos DT. Ischemic but not mechanical preconditioning attenuates ischemia/reperfusion induced myocardial apoptosis in anaesthetized rabbits: the role of Bcl-2 family proteins and ERK1/2. Apoptosis. 2006;11:2195–2204.

[44] Li SX, Cui N, Zhang CL, Zhao XL, Yu SF, Xie KQ. Effect of subchronic exposure to acrylamide induced on the expression of bcl-2, bax and caspase-3 in the rat nervous system. Toxicology. 2006;217:46–53.

[45] Rueda BR, Tilly KI, Botros IW, Jolly PD, Hansen TR, Hoyer PB, Tilly JL. Increased bax and interleukin-1β-converting enzyme messenger ribonucleic acid levels coincide with apoptosis in the bovine corpus luteum during structural regression. Biol Reprod. 1997;56:186–193.

[46] Yadav VK, Lakshmi G, Medhamurthy R. Prostaglandin F2alpha-mediated activation of apoptotic signaling cascades in the corpus luteum during apoptosis: involvement of caspase-activated DNase. J Biol Chem. 2005;18280:10357–10367.

[47] Gürsoy E, Ergin K, Başaloğlu H, Koca Y, Seyrek K. Expression and localisation of Bcl-2 and Bax proteins in developing rat ovary. Res Vet Sci. 2008;84:56–61.

[48] Goyeneche AA, Martinez IL, Deis RP, Gibori G, Telleria CM. In vivo hormonal environment leads to differential susceptibility of the corpus luteum to apoptosis in vitro. Biol Reprod. 2003;68:2322–2330.

[49] Riedlinger G, Okagaki R, Wagner KU, Rucker EB 3rd, Oka T, Miyoshi K, Flaws JA, Hennighausen L. Bcl-x is not required for maintenance of follicles and corpus luteum in the postnatal mouse ovary. Biol Reprod. 2002;66:438–444.

[50] Trott EA, Plouffe L Jr, Hansen K, McDonough PG, George P, Khan I. The role of p53 tumor suppressor gene and bcl-2 protooncogene in rat corpus luteum death. Am J Obstet Gynecol. 1997;177:327–331.

[51] Vaskivuo TE, Ottander U, Oduwole O, Isomaa V, Vihko P, Olofsson JI, Tapanainen JS. Role of apoptosis, apoptosis-related factors and 17beta-hydroxysteroid dehydrogenases in human corpus luteum regression. Mol Cell Endocrinol. 2002;194:191–200.

[52] Dharmarajan AM, Mastroyannis C, Yoshimura Y, Atlas SJ, Wallach EE, Zirkin BR. Quantitative light microscopic analysis of corpus luteum growth during pseudopregnancy in the rabbit. Biol Reprod. 1988;38:863–870.